

Universitat de Girona

MEDICAL IMAGE REGISTRATION AND  
APPLICATIONS

---

Final Project Report  
Image Registration of Chest CT  
Volumes

---

*Students:*

Patricia Cabanillas SILVA  
Ahmed GOUDA  
Zakia KHATUN

*Supervisors:*

Robert MARTÍ  
Nuno GRACIAS



# 1 Introduction

Image registration is the process of aligning two or more sources of data to the same coordinate system. Through all the different registration methods used in medical applications, deformable image registration (DIR) is the one most commonly used [1]. It has many exciting potential applications in diagnostic medical imaging and radiation oncology. The goal of DIR is to find a transformation from one image set to another, such that the differences between the deformed and the target image sets are minimized by providing a voxel-to-voxel deformation matrix.

An application of DIR is exposed in this project, which consists in an image registration of two images from two different times during a breathing cycle (4D CT). So, DIR finds a mapping between a voxel in one phase (e.g., inspiration) to a corresponding voxel in the second phase (e.g., expiration).

For all DIR algorithms, it is highly desirable to provide an estimate of the accuracy of their registration for the desire application [3]. For this project, each data set has associated with it a coordinate list of anatomical landmarks that have been manually identified and registered by an expert in thoracic imaging. The errors would be reported as the Target Registration Error (TRE).

# 2 Dataset

The dataset used for this project is an Inspiratory and Expiratory breath-hold CT image pairs acquired from the National Heart Lung Blood Institute COPDgene study archive [4].

Each available image data set has associated with it a coordinate list of anatomical landmarks that have been manually identified and registered by an expert in thoracic imaging, with repeat registration performed by multiple observers to estimate the spatial variance in feature identification. The point sets contain 300 landmarks points which serve as a reference for evaluating DIR spatial accuracy within the lung for each case. In Figure 1, it is shown an example of the data set used in this project.

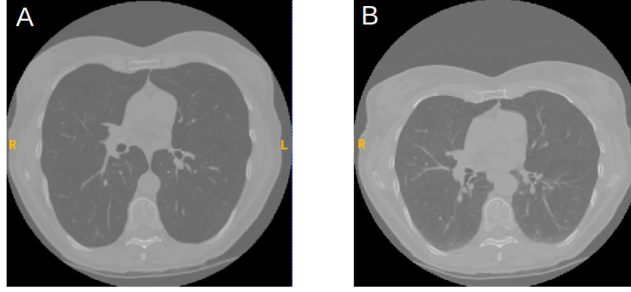


Figure 1: Inhale(A) and Exhale(B) CT image pair of COPD1

### 3 Methodology

The approach we have developed consists of four basic stages. The first step in our pipeline, as shown in Figure 2, is the pre-processing step that is performed to increase the contrast and extract the ROI (lungs).

All the images has a hazy overlay of grayness due to the intensity range were from -2000 to +2600, as shown in image A in Figure 2. To enhance the contrast of the images with this extreme intensity values, we found out that intensity clipping works. The negatives values were clipped and replaced by 0. This brought all the images to have a higher contrast and therefore a better view of the lungs, image B in Figure 2. After contrast enhancement, the next stage was the segmentation. This step was done to extract the lung, and thus remove the surroundings, which damages the results of the registration, image C in Figure 2. This step will be explained with more details in 3.1.

Once that the lungs has been extracted, the next step is the registration of the exhale image(moving) into inhale(fixed). In this step we obtain the deformed exhale image, that has to be similar to the inhale one, and the transform parameters file, where the transformation for each voxel has been saved. Following with the pipeline, the next step is, use the transform parameter file from the registration, to transform the inhale landmark points. These two steps would be explain in detail in 3.2.

Finally, the last step is to calculate the Target Registration Error(TRE), the mean (and standard deviation) 3D Euclidean magnitude distance between

calculated and reference landmark positions.

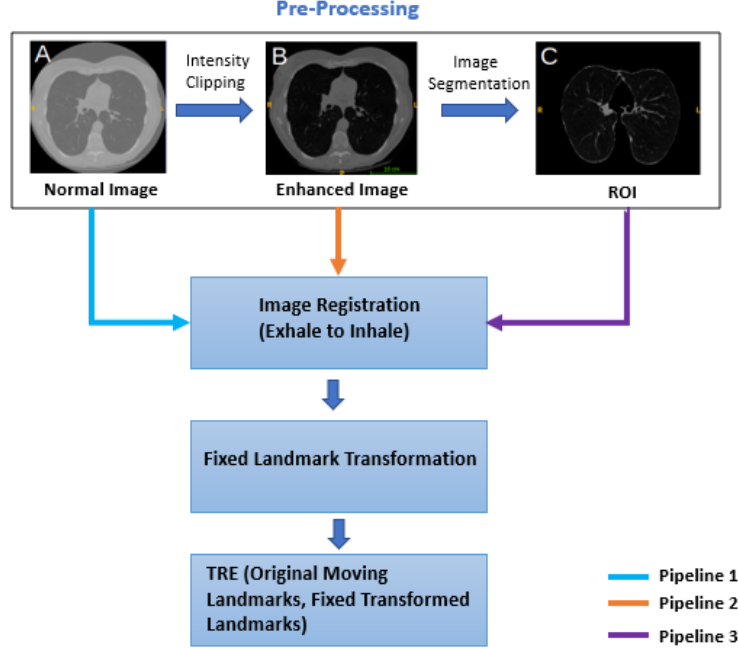


Figure 2: Pipeline of the methodology followed

### 3.1 Image Segmentation and ROI extraction

For image segmentation we should have made previously the clipping step described above. The approach chosen for this task is a 3D region growing algorithm, a *simpleITK* function called *NeighborhoodConnected*. It is similar to 2D region growing in which you select a seed, pixel or group pixels in which a region starts growing. The main difference is in 3D, region grows in volume. In our case, we used two seeds for each lung cavity.

In 3D region growing, removing the trachea is challenging because it is connected to the lungs via bronchi. As a solution, we used 2D watershed segmentation on each slice of the 3D image.

After removing the trachea there are a lot of holes generated because of tissue found in lungs. So, we used morphological operations as dilation and erosion in order to fill all those holes. The output of this is an accurate mask of the lungs. So, the next step would be multiply the mask with the enhanced image to obtain only the lung part.

### 3.2 Image Registration

Image registration is a procedure of finding a spatial deformation to match two images. To accomplish the image registration, we have used Elastix as a software tool to apply 3D registration of moving image on fixed image [6]. The following elastix command line has been used to run the registration.

**elastix -f fixedImage.ext -m movingImage.ext -out outputDirectory  
-p parameterFile.txt**

Here, exhale state has been considered as moving image and inhale as fixed. As parameter file several combinations have been experimented with modification in parameters. The final one which performed the best overall was the combination of affine and bspline transformation with modified parameters.

Using the above mentioned command, we get the transformation file which later has been applied to the fixed landmarks to get output points file containing the input points  $x$  and the transformed points  $T\mu(x)$  and the displacement vector  $T\mu(x) - x$  (in physical coordinates).

We apply the transformation on fixed landmarks even though we register moving image on fixed because in elastix the transformation is defined as a coordinate mapping from the fixed image domain to the moving image domain where transformation is still defined from fixed to moving image. If the transformation would be defined from moving to fixed image, not all voxels in the fixed image domain would be mapped to, and holes would occur in the deformed moving image. To achieve this, the following call has been executed.

**transformix -def inputPoints.txt -out outputDirectory -tp TransformParameters.txt**

The above mentioned command has been used to evaluate the transformation  $T\mu(x)$  at some points  $x \in \Omega_F$ , since the transformation direction is from fixed to moving image.

## 4 Experiments

In general, the affine transformation only captures the global image motion. As a result of this, more useful transformation models are required in the

registration process which are used to make local image deformations. As we are dealing with breath-hold CT images, besides affine transformation, we required to apply non-rigid transformation (bspline) where several parameters have been modified to make the registration works better.

## 4.1 Noiseless/ Less noisy configuration

### 4.1.1 Affine transformation

To register, we are following multi resolution registration as it improves the capture range and robustness of the registration. Under this multi resolution registration category, *RecursiveImagePyramid* has been used which smooths and down samples the image. And to set the multi-resolution strategy, two parameters have been set which are *NumberOfResolutions* and *ImagePyramidSchedule*. The following command lines are executed for setting resolution and image pyramid schedule.

```
(NumberOfResolutions 5)
(ImagePyramidSchedule 16 16 2 8 8 1 4 4 1 2 2 1 1 1 1)
```

In our case, as initially fixed and moving image are not that close so we have used a high number of resolution, this way the images are more blurred and more attention is paid to register large, dominant structures in the beginning. The pyramid schedule defines the amount of blurring in each direction x, y, z and for each resolution level. And as per our data structure, we did not need uniform pyramid schedule so we have used non uniformed pyramid schedule where we have applied less blurring (smoothing) along the z-axis (largest spacing).

As a metric, *AdvancedMattesMutualInformation* has been used as it supports fast computation of the metric value. In this case, we needed to set *NumberOfHistogramBins* which defines number of grey level bins in each resolution level. As we are using a high number of resolution, 64 bins have performed best for us using the following command.

```
(NumberOfHistogramBins 64 )
```

Another important parameter is the sampler as it is responsible for selecting locations in input images for the metric to evaluate positions between voxels. *RandomCoordinate* has been used as it is not limited to voxel positions.

Coordinates between voxels can also be selected. This sampler works well in conjunction with the ***AdaptiveStochasticGradientDescent*** optimiser which requires less parameters to be set and tends to be more robust. And as interpolator, ***FinalBSplineInterpolator*** has been used by higher quality third order B-spline interpolator for generating the resulting deformed moving image. Following command line has been followed.

```
(ResampleInterpolator "FinalBSplineInterpolator")
(FinalBSplineInterpolationOrder 3)
```

#### 4.1.2 B-spline transformation

In B-spline transformation, *RecursiveImagePyramid* has been used, like in affine multi-resolution registration, but this time with a different *NumberOfResolutions* and different *ImagePyramidSchedule*.

```
(NumberOfResolutions 6)
(ImagePyramidSchedule 16 16 2 16 16 2 8 8 1 4 4 1 2 2 1 1 1 1)
```

This time, the number of resolution is bit higher and like before along z-axis, less blurring has been applied. Also, like in affine transformation, *AdvancedMattesMutualInformation* has been used as a metric, using *NumberOfHistogramBins* as 64.

As sampler, *RandomCoordinate*, and optimiser, *AdaptiveStochasticGradientDescent*, has been used. Here in the case of sampler, ***UseRandomSampleRegion*** is set to false so, the sampler draws samples from the entire image domain, the maximum number of sampling attempts value is 50 and ***NumberOfSpatialSamples*** is set to 5000.

Besides these parameters, another important parameter is ***GridSpacingSchedule*** which defines the multiplication factors for all resolution levels. Here, when large grid spacing is chosen then the large structures get matched first and later decreasing the grid spacing is helpful to match the smaller structures. The following command line has been used to set this spacing.

```
(GridSpacingSchedule 16.0 16.0 8.0 4.0 2.0 1.0)
```

## 4.2 Noisy configuration

In our dataset, the second image (COPD2) is comparatively noisy as shown in figure 3, and for this case we tuned some of the previously explained parameters which give better results for noisy cases.

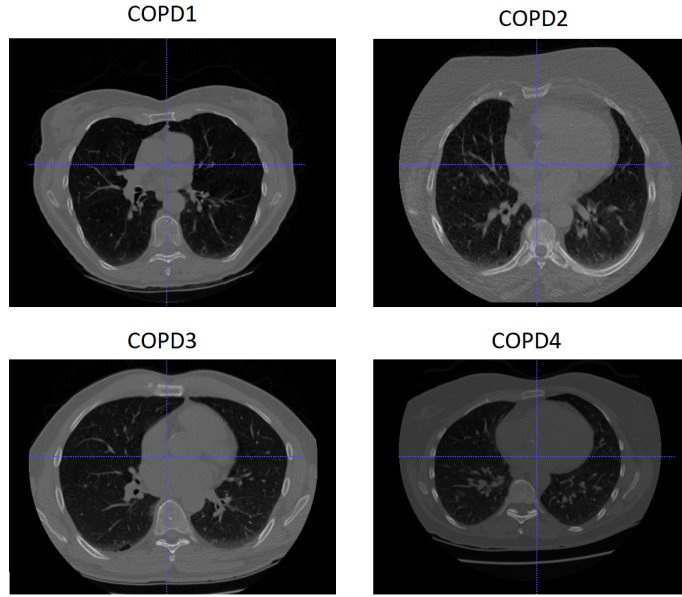


Figure 3: COPD1, COPD2, COPD3 and COPD4 enhanced images

### 4.2.1 B-spline transformation

Additional to previously explained parameters for bspline transformation, here lower *NumberOfResolutions* has been used and also along z-axis lower blurring has been applied (as it is already noisy) using the following command.

```
(NumberOfResolutions 5)  
(ImagePyramidSchedule 16 16 1 8 8 1 4 4 1 2 2 1 1 1 1)
```

Another change in parameter was the *GridSpacingSchedule* which has been used comparatively smaller than before which tries to match comparatively lower structures.

```
(GridSpacingSchedule 8.0 4.0 4.0 2.0 1.0)
```



And as *MaximumNumberOfSamplingAttempts* instead of 50 (for noiseless/less noisy) this time less number of sampling attempts have been taken using the following command line.

(MaximumNumberOfSamplingAttempts 20)

## 5 Result and Analysis

The bar-chart in figure 4 shows a comparison between the Target Registration Error of the normal, enhanced and ROI images registration. In the case of using noisy and noiseless configuration, by removing the negative artifact values from the normal images the TRE error for the enhanced image decreased. Furthermore, segmenting the ROI of lung provides the lowest TRE values for the all the images. Therefore, in this section we will show a comprehensive analysis by applying registration for the ROI images.

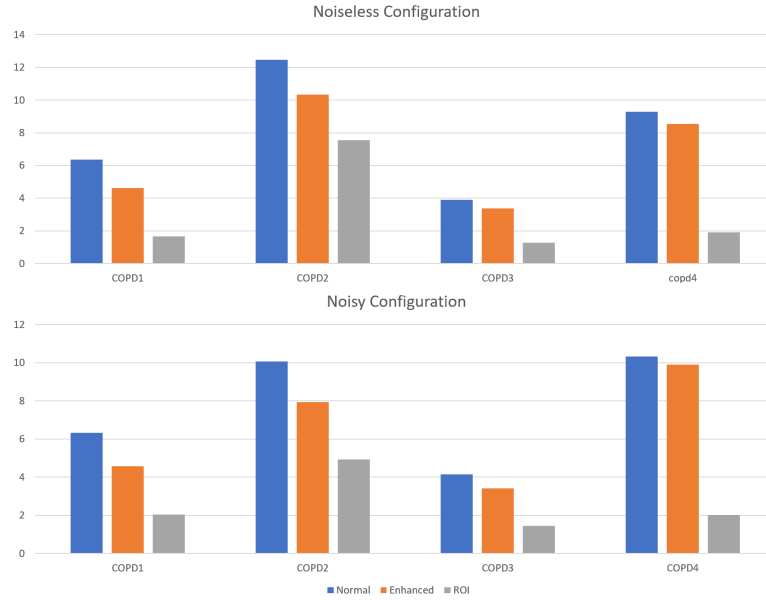


Figure 4: TRE bar-chart for Normal, Enhanced and ROI pipelines

Table 1 demonstrates a quantitative analysis by applying registration for the ROI images using the noisy and noiseless configurations. The lowest registration error is obtained in image COPD3, whereas COPD2 provides the highest registration error. Overall, the noiseless configuration provides the lowest mean and standard deviation registration error in the case of less noisy

images, such as COPD1, COPD3, and COPD4. In contrast, the noisy configuration has the lowest registration error with the noisy image COPD2.

Since the noisy configuration uses a less number of pyramids resolutions, it requires a less registration time in comparison to the noiseless. In addition, the image size has a significant effect on the registration time. When the numbers of pixels per image increase, the registration process requires more computational time.

	Noiseless Configuration			Noisy Configuration		
	mean	std	time(sec.)	mean	std	time(sec.)
<b>COPD1</b>	1.67	1.99	496	2.04	2.53	376
<b>COPD2</b>	7.55	5.49	366	4.94	5.52	339
<b>COPD3</b>	1.28	1.14	452	1.45	1.31	448
<b>COPD4</b>	1.91	1.73	392	2.01	1.79	383

Table 1: The TRE mean, standard deviation and the elapsed time(seconds) for ROI images registration

Figure 5 shows the overlay results for the COPD3 ROI image before and after registration. Using inverse mapping and interpolation, almost all the spatial locations of inhale image are overlapped by moved pixels of the exhale image.

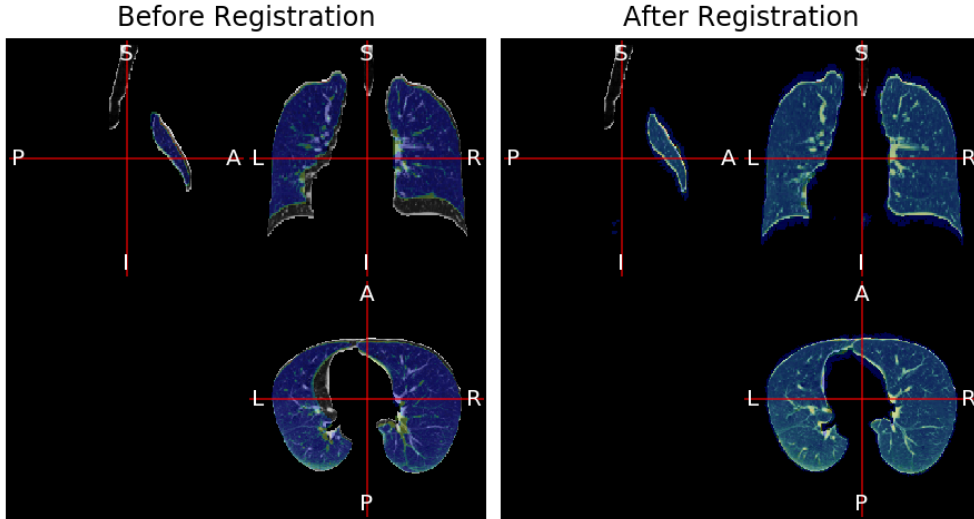


Figure 5: ROI overlay image pair of COPD3 before and after registration

## 6 Conclusion

In this project, we applied non-rigid registration for DIR-Lab CT chest images. We tried different toolboxes, such as Antspy and Elastix. In this report we showed only the results of Elastix, since the TRE error obtained with Antspy was higher than expected. Using a Deep Learning registration techniques (e.g. VoxelMorph [5]) is not an efficient solution because the provided training set includes only four images, while deep learning techniques require a huge data-sets. In contrast, the use of deep learning in future works can help to reduce the execution time of registration.

In our pipeline, we firstly segmented the lung region. Then, we applied multi-resolution affine registration followed by multi-resolution b-spline registration techniques. Tuning the registration hyper-parameters in order to reach the minimum registration error was the most complex task. We conclude that the hyper-parameters configuration is very sensitive to noise level. Thus, we used a different number of pyramid resolution for the noisy COPD2 image. The experimental results shows that we achieved the lowest TRE with the segmented images(ROI). In addition, the image registration process requires more time when the number of pyramid resolution and the number of the pixels of the images increase.

## References

- [1] Sotiras, A., Davatzikos, C., Paragios, N.: Deformable medical image registration: A survey. *IEEE Transactions on Medical Imaging* pp. 1153–1190 (July 2013)
- [2] Ferrante, E., Dokania, P.K., Marini, R., Paragios, N.: Deformable Registration Through Learning of Context-Specific Metric Aggregation, pp. 256–265. Springer International Publishing (2017)
- [3] Janssens G, Jacques L, Orban de Xivry J, Geets X, Macq B. Diffeomorphic registration of images with variable contrast enhancement. *Int J Biomed Imaging*. 2011;2011:891–585.
- [4] Data set available in [www.dir-lab.com](http://www.dir-lab.com)
- [5] G. Balakrishnan, A. Zhao, M. R. Sabuncu, A. V. Dalca and J. Guttag, "An Unsupervised Learning Model for Deformable Medical Image Regis-

tration,” 2018 IEEE/CVF Conference on Computer Vision and Pattern Recognition, Salt Lake City, UT, 2018, pp. 9252-9260.

[6] <http://elastix.isi.uu.nl/download/elastix-5.0.0-manual.pdf>